Unpolarized and Polarized Raman Spectroscopy of Nylon-6 Polymorphs: A Quantum Chemical Approach

Alberto Milani*

Politecnico di Milano, Dip. Chimica, Materiali, Ing. Chimica "G. Natta", Piazza Leonardo da Vinci, 32, 20133, Milano, Italy

Received: December 16, 2014
Revised: February 6, 2015
Published: February 16, 2015

I. INTRODUCTION

Since the beginning of polymer science and technology, vibrational spectroscopic techniques played a significant role in the characterization of the structural properties of polymeric materials, both in pure and applied research.[1−3] Materials science shows that macroscopic properties are often intimately related to the structure of the material and it is in the structural properties that the understanding of the final response of the system must be looked for. This perspective is further required when, as in the case of polymeric materials, the copresence of amorphous and crystalline domains and/or the existence of different polymorphs and/or different morphologies affect the macroscopic properties, implying, for example, a different tensile response, Young modulus, or thermal behavior. In this context, Nylon-6 (NY6) is a very meaningful case, due to the coexistence of two main polymorphs, the α and γ phases, where structure−property relationships are particularly evident.[4] Moreover, these features gain further importance also in connection with the new and promising applications of this polymer, for example, as electrospun nanofibers[5−10] or in nanocomposites.[11,12] In addition to X-ray diffraction techniques, infrared spectroscopy has been widely adopted to characterize NY6 polymorphs,[13−24] and in a recent paper,[25] we revised in detail the assignments and the interpretation of the IR spectra by adopting state-of-the-art density functional theory (DFT) calculations. Raman spectroscopy is a complementary technique with respect to IR spectroscopy, possessing the further advantage of being a nondestructive technique suitable for in situ measurements and without the need of sample preparation. However, some technical difficulties, such as, for example, the less standard and more complicated experimental setup or the problem of sample fluorescence often occurring for commercial polymer samples, prevented its employment in a more technology-oriented environment and limited its application also in fundamental research. Indeed, also in the case of NY6, papers dealing with Raman spectroscopy are much less in number[26−32] with respect to other characterization techniques. However, thanks to the recent improvements in the instrumentation, the context rapidly changed in the past decade, increasing the popularity and the employment of this technique for advanced application in polymer science, as also demonstrated by the present case of NY6.[28−31] Parallel to the experimental investigation and thanks to the advancements in both the computational facilities and available software, molecular modeling has recently become a fundamental tool to support the interpretation of the spectroscopic measurements of polymeric materials[25,33−51] and it is rapidly becoming a tool also for the screening and even design of new interesting systems. In this paper, we employ the recently released version of CRYSTAL14[52,53] code to compute the Raman spectra of NY6 polymorphs. On one hand, our main aim is that of giving a comprehensive spectroscopic characterization of NY6 polymorphs by predicting for the first time their Raman spectra by means of quantum chemical techniques and comparing them with the available experimental data. Due to the interplay between several intramolecular and intermolecular effects (hydrogen bonding and van der Waals packing interactions), this is an ideal case to

test the accuracy of theory in describing these structural phenomena and their effect on the final spectroscopic response. Moreover, we want to assess the general application of state-of-the-art computational tools for the prediction of polarized Raman spectra of single crystal polymers by using NY6 as a test case. The possibility to predict with good accuracy polarized spectra of a crystal characterized by a given orientation could be of great help for the interpretation of experimental polarized Raman spectra taken for an oriented sample, e.g., for the assessment of the degree and kind of polymer orientation in real anisotropic samples, as, for instance, stretch oriented polymer samples, polymer fibers, etc.

II. COMPUTATIONAL DETAILS

Raman spectra of the α and γ forms of NY6 have been computed in the framework of DFT by using periodic boundary conditions and employing the CRYSTAL14 software.[52−55] In recent years, this software proved to be very effective in the prediction of the structure and IR spectra of crystalline polymers, as reported in different papers.[44−51] The previous version of this code has been adopted in a recent paper[25] to fully optimize the crystal structure of NY6 polymorphs and to calculate their IR spectra. In that work, the B3LYP[56,57] hybrid exchange-correlation functional has been adopted together with 6-31G(d,p) basis set and introducing Grimme's correction for dispersion interactions.[58−60] Even if this correction is of semiempirical nature and does not take into account many body effects,[61−63] it was revealed to be accurate enough for a very reliable description of the energetic, structural, and spectroscopic properties of molecular crystals. In the present investigation, we adopted the combination (B3LYP-D/6-31G(d,p)) to predict the Raman response, starting from the optimized geometries determined in ref 25, to which we refer for further details and structural data. In Figure 1, the structures so obtained are sketched: in the case of the α form, a transplanar (fully extended) conformation is found for the chains which form sheets of hydrogen bonded molecules; on the other hand, the γ form is characterized by a skew conformation of the CH_2 units adjacent to the amide group, determining a nonplanar arrangement of the backbone atoms.

The total Raman intensity for each normal mode Q_n is calculated referring to an ideal experiment on a polycrystalline powder sample (i.e., not oriented) by collecting the scattered radiation in all the directions of polarization

$$I_{tot}(n) \propto (45\bar{\alpha}(n)^2 + 7\gamma(n)^2) \quad (1)$$

with invariants defined as $\bar{\alpha}(n) = (1/3)(\alpha_{xx}(n) + \alpha_{yy}(n) + \alpha_{zz}(n))$ and $\gamma(n)^2 = (1/2)[(\alpha_{xx}(n) - \alpha_{yy}(n))^2 + (\alpha_{yy}(n) - \alpha_{zz}(n))^2 + (\alpha_{zz}(n) - \alpha_{xx}(n))^2 + 6(\alpha_{xy}^2(n) + \alpha_{yz}^2(n) + \alpha_{zx}^2(n))]$, where $\alpha_{ij}(n) = \boldsymbol{\alpha}(n, i, j)$ is the i,j-th component of the Raman tensor relative to the normal mode Q_n (i.e., the derivative of the components of the polarizability tensor with respect to the normal coordinate Q_n).[64,65]

In addition to total Raman intensities, CRYSTAL14 computes also the single crystal directional Raman intensities defined as

$$I_{ij}(n) = V^*\boldsymbol{\alpha}(n, i, j)^2 \quad (2)$$

where V is the cell volume. The intensities I_{ij} are the intensities which could be obtained in an ideal experiment on a single crystal by using incident radiation polarized in the i direction and collecting scattered radiation in the j direction. The Raman tensor and directional intensities have been used to discuss and compute the polarized Raman spectra of the system investigated.

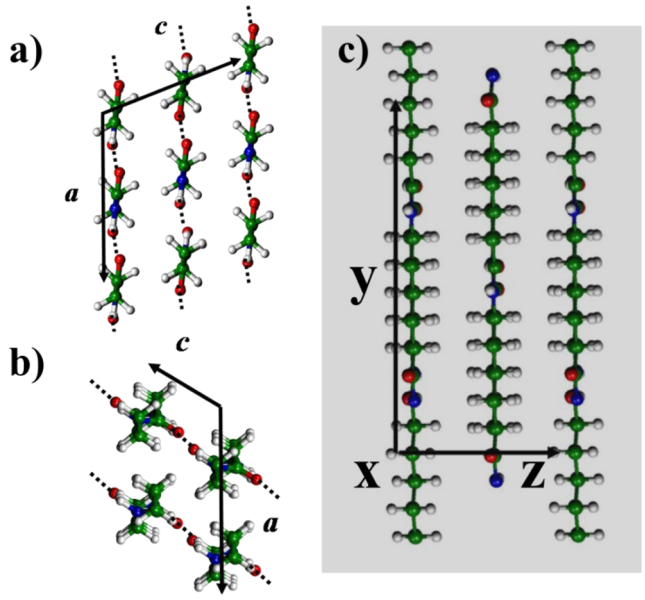

Figure 1. Sketches of the crystalline structures of the α (panels a and c) and γ polymorphs (panel b) of Nylon-6. Carbon atoms are in green, hydrogen atoms in white, oxygen atoms in red, and nitrogen atoms in blue; hydrogen bonds are marked with dots. In panel c, the convention adopted for the x, y, z axis is indicated: for both polymorphs, the chain axis corresponds to the y axis, while x and z are lying, respectively, parallel and perpendicular to the plane of the molecular sheets defined by the carbon backbones of adjacent H-bonded polymer chains.

The spectra so obtained are compared with the experimental Raman spectra reported in the literature. In particular, unpolarized Raman spectra of α and γ phases have been taken by ref 29 (very similar spectra are also reported in ref 28), while polarized Raman spectra of the α form relative to stretch-oriented samples are taken from ref 27. As usual in computational vibrational spectroscopy, in order to take into account the effects due to the neglect of anharmonicity, to the approximated treatment of electron correlation and to the finiteness of the basis sets, frequency scaling factors are introduced when comparing the DFT computed and experimental data.[66] To this aim, the calculated frequencies here reported have been scaled by using the standard scaling factor of 0.9614 reported by Merrick et al.[66] Tables reporting unscaled frequency values and total and directional Raman intensities of the two polymorphs are reported in the Supporting Information.

In addition to the prediction of the Raman spectra of the crystal, we computed also the Raman spectra for the infinite regular polymer chains having, respectively, the same conformation observed in the crystal. These spectra give the possibility to discuss briefly the effect of crystal packing and intermolecular interaction on the Raman response (see next section). Also, in this case, the starting geometries are the optimized ones reported in ref 25.

III. RESULTS AND DISCUSSION

III.1. Unpolarized Raman Spectra of α and γ Phases.

Among the few papers dealing with Raman spectroscopy, only

in two of them,[28,29] the Raman spectra of α and γ polymorphs have been compared with the aim of finding spectroscopic markers of one form or the other. In Table 1, a summary of the frequencies of the unambiguous marker bands proposed are reported, together with the values obtained by DFT calculations (see next discussion).

Table 1. List of the Frequency Values (cm^{-1}) of Unambiguous Marker Bands Proposed by Previous Authors[28,29] for the α and γ Polymorphs of NY6 and Corresponding DFT Computed (B3LYP-D/6-31G(d,p)) Values (Computed Frequencies Are Scaled by 0.9614)[a]

α-NY6		γ-NY6	
expt[28,29]	DFT (scaled)	expt[28,29]	DFT (scaled)
1130	1112	962/977	948
1470	1478	1080	1057
1480	1481		
1203	**1183**	1234	**1217**
~1420	**1412**		

[a]The frequency values of new marker bands proposed on the basis of the calculations are reported in boldface.

In Figure 2, the experimental[29] and DFT computed spectra of the two polymorphs are compared in the spectral range 1800−800 cm^{-1}.

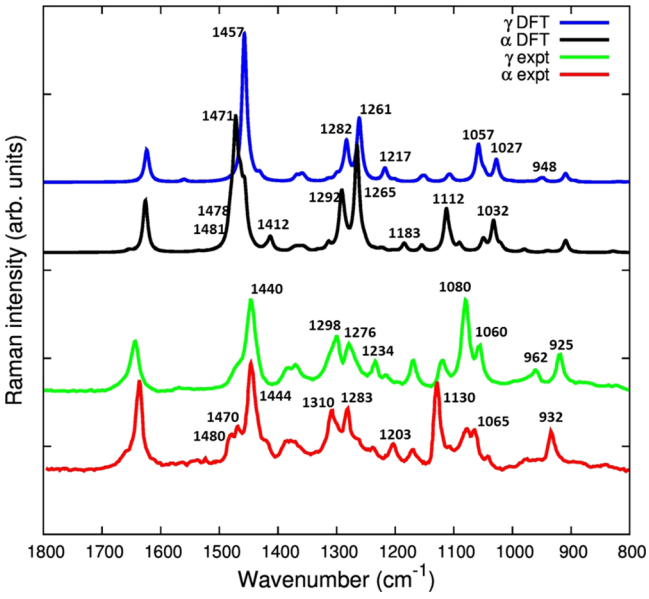

Figure 2. Comparison between experimental[29] and DFT computed (B3LYP-D/6-31G(d,p)) Raman spectra of α and γ polymorphs. The predicted frequency values have been scaled by 0.9614 for a better comparison with the experimental spectra.

The agreement between experimental and DFT computed spectra is impressive also in the minor details. Apart from the prediction of the spectral features of each polymorph, the significant advantage of a combined computational/experimental approach relies in the possibility of using spectroscopy to give an unambiguous characterization of polymorphism effects, as discussed in detail in the following.

Starting from the lower frequencies, a band is found at 925 cm^{-1} for γ-NY6 and has been proposed in ref 28 as a possible marker of this phase; however, due to the presence of a band at 932 cm^{-1} for α-NY6 and based on DFT calculations where both crystals present a line in this range, it is evident that such a band cannot be confidently taken as a marker of one phase only. On the other hand, the band observed[28] at 962 cm^{-1} (977 cm^{-1} in ref 31) for γ-NY6 is indeed a good marker band, as demonstrated by the computation where the band predicted at 948 cm^{-1} (CH_2 twisting + CONH in plane) has no counterparts in the α crystal, apart from a very weak feature. Around 1100 cm^{-1}, the experimental spectra present a pattern where significant differences are found between the two polymorphs. Some authors[29,31] proposed the band at 1065 cm^{-1} as a marker of α-NY6: the comparison with γ-NY6, having a band at 1060 cm^{-1}, and with the calculations where two bands of comparable intensity are predicted at 1032 and 1027 cm^{-1} (CC stretching + CH_2 wagging) for α and γ crystals, respectively, does not allow this feature to be considered as a reliable marker. Instead, a band at 1080 cm^{-1} is dominant for γ-NY6, as also demonstrated by the predicted spectra: an intense band is present for the γ crystal at 1057 cm^{-1} (CC stretching + CH_2 twisting), while α possesses a much weaker band in the same region, in agreement with the lower intensity observed for the experimental 1080 cm^{-1} band. On the other hand, the opposite behavior is observed for the band measured at 1130 cm^{-1}, very intense for α-NY6 and much weaker for γ-NY6 (found at 1121 cm^{-1}). Again, DFT calculations nicely reproduce the experimental observation: the α crystal shows a feature at 1112 cm^{-1} (CC stretching + CH_2 wagging), while at similar frequencies the γ crystal possesses a weaker contribution. We can thus conclude that in this range the 1080 and 1130 cm^{-1} can be taken as reliable marker bands of γ and α polymorphs, respectively. At larger frequency values, some interesting observations can be done on the basis of the results of the computations: while the experimental band at 1170 cm^{-1} observed for both polymorphs is indeed computed for both of them, the two bands at 1203 cm^{-1} for α-NY6 and at 1234 cm^{-1} for γ-NY6, overlooked in previous investigations, can be taken, respectively, as marker bands of the two polymorphs. Indeed, the 1203 cm^{-1} is predicted at 1183 cm^{-1} (CH_2 wagging) for the α crystal and the 1234 cm^{-1} band is predicted at 1217 cm^{-1} (CH_2 twisting) for the γ crystal, while α shows only a very weak line close in frequency, consistently with a weak band observed at 1238 cm^{-1}.

Both polymorphs show two bands around 1300 cm^{-1} (1283−1310 cm^{-1} for α-NY6 and 1276−1298 cm^{-1} for γ-NY6) which have been proposed by different authors as possible spectroscopic markers. Indeed, in ref 27, the 1283 cm^{-1} band is taken as a marker of α-NY6, while, in ref 29, the same phase is associated with the 1310 cm^{-1}; moreover, in ref 28, the band at 1298 cm^{-1} is considered as a marker of γ-NY6. It is already evident from the experimental spectra that the similarities between the two polymorphs in this range do not allow these bands to be considered as reliable markers based only on small differences in frequency values or relative intensities. This is further supported by DFT calculations: both crystals do possess two bands in this region, 1265−1292 cm^{-1} for the α crystal (CH_2 twisting) and 1261−1282 cm^{-1} for the γ crystal (CH_2 twisting). The 1265 cm^{-1} band shows a larger intensity in the α phase (as also measured experimentally), but this is not enough to consider it as an unambiguous marker. It is interesting to notice that DFT calculations allow a further possible marker band to be identified for the α crystal as the shoulder on the lower frequency side of the experimental band at 1444 cm^{-1}: a contribution is indeed computed at 1412 cm^{-1}

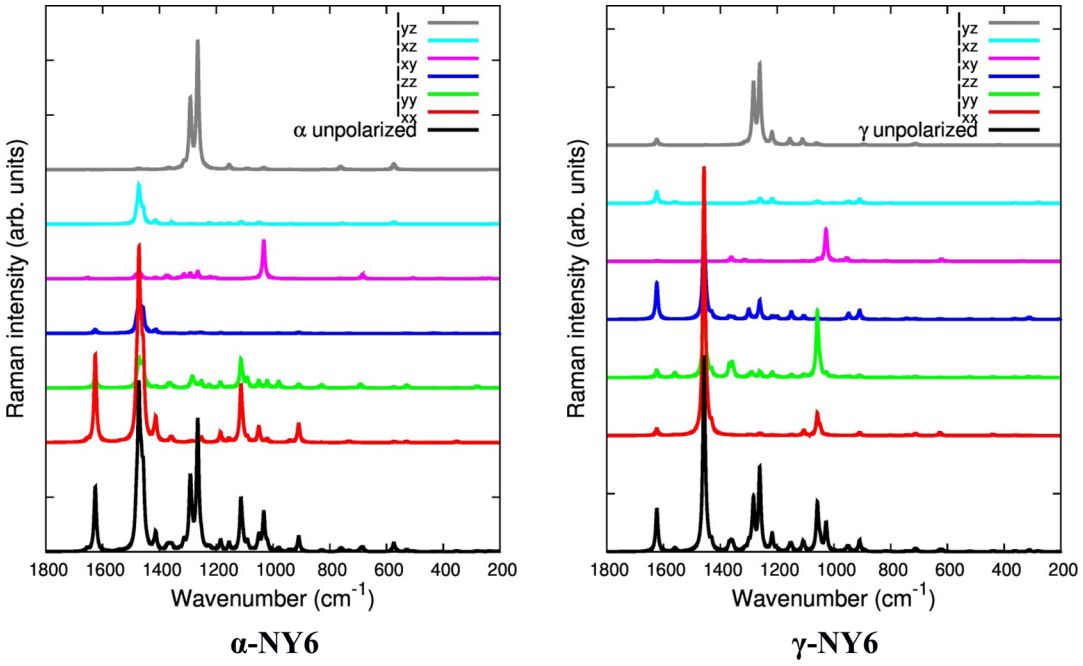

Figure 3. DFT computed unpolarized Raman spectra compared with the spectra obtained on the basis of the different directional Raman intensities. Frequency values are scaled by 0.9614.

(CH_2 bending) and explains the differences observed in the spectra. Finally, it has been proposed that the bands measured at 1470 and 1480 cm^{-1} for α-NY6 can be considered as reliable markers. From the computations, it appears that only one band is predicted at 1471 cm^{-1}. On the other hand, a closer look to the results of the calculations shows that, in addition to the 1471 cm^{-1} band, also two other Raman transitions are predicted at 1478 and 1481 cm^{-1} (CH_2 bending) for the α crystal, which merge in a single (calculated) band due to the bandwidth adopted to plot the computed spectrum; in the case of the γ crystal, no contributions are computed on the higher frequency side of the 1457 cm^{-1} band (see also numerical data in the Supporting Information). Therefore, apart from the smaller differences in relative frequencies, this result seems to justify the assignment of the experimental bands at 1470 and 1480 cm^{-1} as markers of α-NY6. On the basis of the above discussion, the experimental and DFT computed frequencies of the unambiguous marker bands are summarized in Table 1.

On the basis of the results reported, we can conclude that DFT calculations appear to be mandatory for a detailed Raman characterization of NY6 polymorphs and related marker bands: only thanks to these computations, it has been possible to obtain an unambiguous description where some of the previous proposed marker bands have been confirmed, other ones rejected and new ones suggested. Such a clear description is required to fully exploit the power of vibrational spectroscopy in the context of polymer structure characterization.

As a final test, in Figure SI1 of the Supporting Information, the Raman spectra computed for regular one-dimensional chain models are also reported in order to show the effects of intermolecular interactions. Even if the differences with respect to the spectra computed for the crystals are less pronounced than in the case of the IR spectra,[25] it can be verified that the one-dimensional models are not suitable for the correct prediction of the experimental Raman spectra. The occurrence of hydrogen bonding between neighboring chains modulates significantly the frequencies of many bands and the general pattern of the spectrum, implying that the correct description of intermolecular interactions (i.e., considering the whole 3D crystal instead of an isolated 1D model chain) is mandatory for a reliable interpretation of the spectra.

III.2. Polarized Raman Spectra. In addition to the Raman spectra predicted for isotropic samples, built by taking into account the suitable Raman intensities, it is possible to verify the dependence from the crystal orientation and experimental setup of the Raman spectra, by considering the directional intensities defined by eq 2 and calculated on the basis of individual components of the Raman tensor. These results give a powerful description of the polarization properties of NY6 polymorphs, allowing the result to be predicted that would be observed in a polarized Raman measurement on real samples showing preferential orientation. Polarized Raman spectroscopy presents some peculiarities and advantages that make it an important technique in the context of polymer spectroscopy: from a fundamental point of view, it allows a detailed assignment of the bands observed to be carried out in terms of symmetry, thus permitting one to discriminate between different chain conformations based on their different symmetry selection rules; on the other hand, it can give significant information on the anisotropy of oriented polymer samples, such as, for example, electrospun NY6 nanofibers.[5−10,29,31]

In Figure 3, the DFT computed Raman spectra discussed in the previous section are compared to the individual Raman spectra built by taking into account the different directional intensities.

For both polymorphs, the choice adopted for the *x*, *y*, and *z* axis is reported in Figure 1.

It is quite evident that both phases present evident anisotropic scattering properties, and it is useful to focus in particular on three main spectral regions: (i) the 1800−1400 cm^{-1}, (ii) the 1300−1200 cm^{-1}, and (iii) the 1200−800 cm^{-1} regions. In the case of region i, it is immediate to verify that in the α form the two intense bands are mainly generated by the

xx component of the Raman tensor and a similar behavior is shown in region iii by the bands at 1112 cm^{-1} and at about 900 cm^{-1}; on the other hand, the band at 1032 cm^{-1} is mainly related to the *xy* component, while the most selective trend is shown in region ii by the pair of bands at 1292 and 1265 cm^{-1} which are practically due only to the *yz* directional intensity. In the case of the γ form, the intense band in region i now takes significant contribution by all the diagonal components of the Raman tensor, while that at about 1600 cm^{-1} is now related only to the *zz* component. A similar behavior is shown also in region iii where the intense band at 1057 cm^{-1} is related to the *yy* and *xx* components, while the band at 1027 cm^{-1} is generated uniquely by *xy* intensity. Again, also for the γ form, the doublet of intense bands in region ii is related almost exclusively to *yz* intensity.

The spectra reported in Figure 3 already give significant information about the directional Raman properties of NY6 polymorphs, but they cannot be directly compared to the spectra obtained by polarized Raman experiments. Indeed, on the basis of the symmetry properties of the system, its orientation, the setup, and the geometry of the experiment, the polarized spectra obtained are related to a specific combination of the different directional components. In ref 27, polarized Raman measurements of a stretch oriented sample of NY6 in the α form have been presented and the relationship between the experimental setup A(BC)D (A = propagation direction of the incident radiation, B = direction of polarization of incident radiation, C = direction of polarization of analyzed radiation, D = propagation direction of scattered radiation) and the proper combination of the molecular polarizability ($\boldsymbol{\alpha}$) components leading to the Raman spectrum has been reported. Four cases are analyzed: $X(YY)Z$ geometry corresponding to α_{yy}^2 in our system of axis, $X(YX)Z$ and $X(ZY)Z$ polarizations corresponding to $^1/_2(\alpha_{yz}^2 + \alpha_{xy}^2)$ and $X(ZX)Z$ polarization corresponding to $^1/_8(\alpha_{zz} - \alpha_{xx})^2 + {}^1/_2\alpha_{zx}^2$.

In Figure 4, the experimental polarized spectra reported for these four different cases are compared to the theoretical spectra where the intensities are calculated on the basis of the DFT computed Raman tensor and on the proper combination of the directional Raman intensities shown in Figure 3.

The comparison reveals a very good agreement: the DFT computed spectrum reproduces the experimental one even in the finer details, and the only minor discrepancies are the relative intensities of the main bands for the spectrum with $X(YX)Z$ polarization, slightly overestimated by DFT calculations. However, a not completely perfect orientation of the sample with respect to the directional components cannot be excluded and could play a role in explaining possible minor differences with respect to computations.

As already mentioned, polarized measurements allowed to assign the bands observed in the spectra based on their symmetry properties: Figure 4 demonstrated without any doubt that the state-of-the-art computational method can support these experimental measurements, giving a very precise and unambiguous description of anisotropic properties, further enhancing the power of a combined experimental/computational approach to carry out a detailed spectroscopic characterization of polymer materials.

IV. CONCLUSIONS

In this paper, we presented for the first time the application of state-of-the-art periodic DFT calculations for the prediction of the Raman spectra of NY6 polymorphs. The comparison with

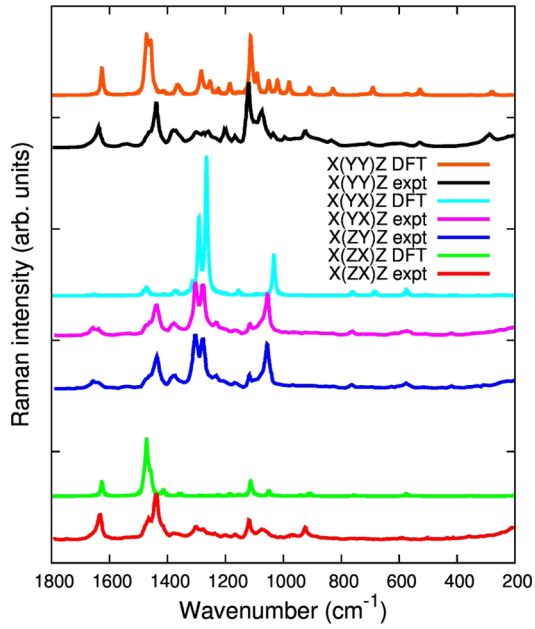

Figure 4. Comparison between experimental polarized Raman spectra of the α-NY6 obtained with different experimental polarizations (taken from ref 27) and corresponding Raman spectra obtained by the DFT computed (B3LYP-D/6-31G(d,p)) Raman tensors (see text for the correspondence between experimental geometry and "active" molecular polarizability components). DFT computed frequencies are scaled by 0.9614. $X(YX)Z$ and $X(ZY)Z$ polarizations both correspond to $^1/_2(\alpha_{yz}^2 + \alpha_{xy}^2)$, and thus, in the figure, only one corresponding theoretical spectrum (indicated as "$X(YX)Z$ DFT") is reported for a comparison.

the experimental spectra reveals the high accuracy and predictive power of the computational methodology adopted, allowing a precise assignment and interpretation of the Raman spectra of both α and γ phases and giving an unambiguous characterization of these polymorphs through their spectral markers. Such a straightforward description is not possible based only on an experimental approach, as demonstrated by the ambiguous and debated assignments which can be usually found in the literature for many different polymeric materials. Very few Raman spectroscopic studies of NY6 polymorphs have been presented up to now, and the present results are particularly meaningful and novel in this context, since they give new insights on the vibrational response of these systems, offering a possible contribution for the characterization of innovative nylon-based systems. Indeed, these findings pave the way to the application of computational Raman spectroscopy in different branches of polymer science and technology: as in the case of IR spectroscopy, characterization tools are required not only to study the structural evolution in peculiar systems (e.g., electrospun nanofibers), but they can be used also for analytical and quantitative measurements in more technological environments. The complementary information given by IR and Raman spectroscopies, now both supported by computation tools, is significant in this context.

Moreover, the successful prediction of polarized Raman spectra further enhances the potentialities of these computational tools in the more general context of advanced polymer materials, pointing out how a combined computational/experimental approach is mandatory for a straightforward characterization of anisotropic polymer samples by means of Raman spectroscopy.

ASSOCIATED CONTENT

Supporting Information

Figure with the comparison between experimental and DFT computed spectra of the α and γ crystals and one-dimensional, infinite single chain models; tables reporting DFT computed (B3LYP-D/6-31G(d,p)) unscaled frequency values, total and directional Raman intensities of the NY6 α and γ polymorphs.

AUTHOR INFORMATION

Corresponding Author

*E-mail: alberto.milani@polimi.it.

Notes

The authors declare no competing financial interest.

ACKNOWLEDGMENTS

The author would like to gratefully thank Chiara Castiglioni (POLIMI) for the useful discussion and suggestions during the writing of the manuscript.

REFERENCES

(1) Painter, P. C.; Coleman, M. M.; Koening, J. L. *The theory of vibrational spectroscopy and its application to polymeric materials*; Wiley: Chichester, U.K., 1982.

(2) Zerbi, G. In *Advances in Infrared and Raman spectroscopy*; Clark, R. J. H., Hester, R. R., Eds.; Wiley: New York, 1984; Vol. *11*, p 301.

(3) Castiglioni, C. In *Vibrational Spectroscopy of Polymers: Principles and Practices*; Everall, N. J., Chalmers, J. M., Griffiths, P. R., Eds.; Wiley: Chichester, U.K., 2007; p 455.

(4) Kohan, M. I. *Nylon Plastics Handbook*; Hanser: New York, 1995.

(5) Lee, K. H.; Kim, K. W.; Pesapane, A.; Kim, H. Y.; Rabolt, J. F. Polarized FT-IR Study of Macroscopically Oriented Electrospun Nylon-6 Nanofibers. *Macromolecules* **2008**, *41*, 1494−1498.

(6) Granato, F.; Bianco, A.; Bertarelli, C.; Zerbi, G. Composite Polyamide 6/Polypyrrole Conductive Nanofibers. *Macromol. Rapid Commun.* **2009**, *30*, 453−458.

(7) Bianco, A.; Iardino, G.; Manuelli, A.; Bertarelli, C.; Zerbi, G. Strong Orientation of Polymer Chains and Small Photochromic Molecules in Polyamide 6 Electrospun Fibers. *ChemPhysChem* **2007**, *8*, 510−514.

(8) Liu, Y.; Qi, L.; Guan, F.; Hedin, N. E.; Zhu, L.; Fong, H. Crystalline Morphology and Polymorphic Phase Transitions in Electrospun Nylon 6 Nanofibers. *Macromolecules* **2007**, *40*, 6283−6290.

(9) Zussman, E.; Burman, N.; Yarin, A. L.; Khalfin, R.; Cohen, Y. Tensile Deformation of Electrospun Nylon-6,6 Nanofibers. *J. Polym. Sci., Part B: Polym. Phys.* **2006**, *44*, 1482−1489.

(10) Stachewicz, U.; Barber, A. H. Enhanced Wetting Behavior at Electrospun Polyamide Nanofiber Surfaces. *Langmuir* **2011**, *27*, 3024−3029.

(11) Loo, L. S.; Gleason, K. K. Fourier Transform Infrared Investigation of the Deformation Behavior of Montmorillonite in Nylon-6/Nanoclay Nanocomposite. *Macromolecules* **2003**, *36*, 2587−2590.

(12) Chen, G.; Shen, D.; Feng, M.; Yang, M. An Attenuated Total Reflection FT-IR Spectroscopic Study of Polyamide 6/Clay Nanocomposite Fibers. *Macromol. Rapid Commun.* **2004**, *25*, 1121−1124.

(13) Murthy, N. S.; Bray, R. G.; Correale, S. T.; Moore, R. A. F. Drawing and Annealing of Nylon-6 Fibres: Studies of Crystal Growth, Orientation of Amorphous and Crystalline Domains and Their Influence on Properties. *Polymer* **1995**, *36*, 3863−3873.

(14) Loo, L. S.; Gleason, K. K. Insights into Structure and Mechanical Behavior of α and γ Crystal Forms of Nylon-6 at Low Strain by Infrared Studies. *Macromolecules* **2003**, *36*, 6114−6126.

(15) Vasanthan, N.; Salem, D. R. FTIR Spectroscopic Characterization of Structural Changes in Polyamide-6 Fibers During Annealing and Drawing. *J. Polym. Sci., Part B: Polym. Phys.* **2001**, *39*, 536−547.

(16) Na, B.; Lv, R.; Tian, N.; Xu, W.; Li, Z.; Fu, Q. Micro-FT-IR Study of Stretching a Single Filament: Polymorphic Transition in Nylon 6. *J. Polym. Sci., Part B: Polym. Phys.* **2009**, *47*, 898−902.

(17) Vasanthan, N. Orientation and Structure Development in Polyamide 6 Fibers Upon Drawing. *J. Polym. Sci., Part B: Polym. Phys.* **2003**, *41*, 2870−2877.

(18) Miri, V.; Persyn, O.; Lefebvre, J. M.; Segula, R.; Stroeks, A. Strain-Induced Disorder−Order Crystalline Phase Transition in Nylon 6 and its Miscible Blends. *Polymer* **2007**, *48*, 5080−5087.

(19) Miyake, A. Infrared Spectra and Crystal Structures of Polyamides. *J. Polym. Sci.* **1960**, *44*, 223−232.

(20) Sandeman, I.; Keller, A. Crystallinity Studies of Polyamides by Infrared, Specific Volume and X-Ray Methods. *J. Polym. Sci.* **1956**, *19*, 401−435.

(21) Rotter, G.; Ishida, H. FTIR Separation of Nylon-6 Chain Conformations: Clarification of the Mesomorphous and γ-Crystalline Phases. *J. Polym. Sci., Part B: Polym. Phys.* **1992**, *30*, 489−495.

(22) Vasanthan, N. Determination of Molecular Orientation of Uniaxially Stretched Polyamide Fibers by Polarized Infrared Spectroscopy: Comparison of X-Ray Diffraction and Birefringence Methods. *Appl. Spectrosc.* **2005**, *59*, 897−903.

(23) Persyn, O.; Miri, V.; Lefebvre, J. M.; Depecker, C.; Gors, C.; Stroeks, A. Structural Organization and Drawability in Polyamide Blends. *Polym. Eng. Sci.* **2004**, *44*, 261−271.

(24) Vasanthan, N.; Murthy, N. S.; Bray, R. G. Investigation of Brill Transition in Nylon 6 and Nylon 6,6 by Infrared Spectroscopy. *Macromolecules* **1998**, *31*, 8433−8435.

(25) Quarti, C.; Milani, A.; Civalleri, B.; Orlando, R.; Castiglioni, C. Ab Initio Calculation of the Crystalline Structure and IR Spectrum of Polymers: Nylon 6 Polymorphs. *J. Phys. Chem. B* **2012**, *116*, 8299−8311.

(26) Schmidt, P.; Hendra, P. J. The Application of Fourier-Transform Raman Spectroscopy to the Determination of Conformation in Poly(ε-caprolactam) Chains. *Spectrochim. Acta, Part A* **1994**, *50*, 1999−2004.

(27) Song, K.; Rabolt, J. F. Polarized Raman Measurements of Uniaxially Oriented Poly(ε-caprolactam). *Macromolecules* **2001**, *34*, 1650−1654.

(28) Ferreiro, V.; Depecker, C.; Laureyns, J.; Coulon, G. Structures and Morphologies of Cast and Plastically Strained Polyamide 6 Films as Evidenced by Confocal Raman Microspectroscopy and Atomic Force Microscopy. *Polymer* **2004**, *45*, 6013−6026.

(29) Stephens, J. S.; Chase, D. B.; Rabolt, J. F. Effect of the Electrospinning Process on Polymer Crystallization Chain Conformation in Nylon-6 and Nylon-12. *Macromolecules* **2004**, *37*, 877−881.

(30) Bellan, L. M.; Craighead, H. G. Molecular Orientation in Individual Electrospun Nanofibers Measured Via Polarized Raman Spectroscopy. *Polymer* **2008**, *49*, 3125−3129.

(31) Giller, C. B.; Chase, D. B.; Rabolt, J. F.; Snively, C. M. Effect of Solvent Evaporation Rate on the Crystalline State of Electrospun Nylon 6. *Polymer* **2010**, *51*, 4225−4230.

(32) Shukla, S. K.; Kumar, N.; Tandom, P.; Gupta, V. D. Vibrational dynamics of gamma form of nylon 6 (γNY6). *J. Appl. Polym. Sci.* **2010**, *116*, 3202−3211.

(33) Koglin, E.; Meier, R. Conformational Dependence of Raman Frequencies and Intensities in Alkanes and Polyethylene. *Comput. Theor. Polym. Sci.* **1999**, *9*, 327−333.

(34) Meier, R. J. Studying the Length of Trans Conformational Sequences in Polyethylene Using Raman Spectroscopy: a Computational Study. *Polymer* **2002**, *43*, 517−522.

(35) Tarazona, A.; Koglin, E.; Coussens, B. B.; Meier, R. J. Conformational Dependence of Vibrational Frequencies and Intensities in Alkanes and Polyethylene. *Vib. Spectrosc.* **1997**, *14*, 159−170.

(36) Milani, A.; Castiglioni, C.; Di Dedda, E.; Radice, S.; Canil, G.; Di Meo, A.; Picozzi, R.; Tonelli, C. Hydrogen Bonding Effects in

Perfluorinated Polyamides: An Investigation Based on Infrared Spectroscopy and Density Functional Theory Calculations. *Polymer* **2010**, *51*, 2597−2610.
(37) Milani, A.; Tommasini, M.; Castiglioni, C.; Zerbi, G.; Radice, S.; Canil, G.; Toniolo, P.; Triulzi, F.; Colaianna, P. Spectroscopic Studies and First-Principles Modelling of 2,2,4-trifluoro-5-trifluoromethoxy-1,3-dioxole (TTD) and TTD−TFE Copolymers (Hyflon® AD). *Polymer* **2008**, *49*, 1812−1822.
(38) Radice, S.; Di Dedda, E.; Tonelli, C.; Della Pergola, R.; Milani, A.; Castiglioni, C. FT-IR Spectroscopy and DFT Calculations on Fluorinated Macromer Diols: IR Intensity and Association Properties. *J. Phys. Chem. B* **2010**, *114*, 6332−6336.
(39) Milani, A.; Zanetti, J.; Castiglioni, C.; Di Dedda, E.; Radice, S.; Canil, G.; Tonelli, C. Intramolecular and Intermolecular OH···O and OH···F Interactions in Perfluoropolyethers with Polar End Groups: IR Spectroscopy and First-Principles Calculations. *Eur. Polym. J.* **2012**, *48*, 391−403.
(40) Nakhmanson, S. M.; Korlacki, R.; Travis Johnston, J.; Ducharme, S.; Ge, Z.; Takacs, J. M. Vibrational Properties of Ferroelectric β-Vinylidene Fluoride Polymers and Oligomers. *Phys. Rev. B* **2010**, *81*, 174120.
(41) Kleis, J.; Lundqvist, B. I.; Langreth, D. C.; Schroder, E. Towards a Working Density-Functional Theory for Polymers: First-Principles Determination of the Polyethylene Crystal Structure. *Phys. Rev. B* **2007**, *76l*, 100201.
(42) Ramer, N. J.; Marrone, T.; Stiso, K. A. Structure and Vibrational Frequency Determination for α-Poly(vinylidene fluoride) Using Density-Functional Theory. *Polymer* **2006**, *47*, 7160−7165.
(43) Ramer, N. J.; Raynor, C. M.; Stiso, K. A. Vibrational Frequency and LO−TO Splitting Determination for Planar−Zigzag β-poly-(vinylidene fluoride) Using Density-Functional Theory. *Polymer* **2006**, *47*, 424−428.
(44) Torres, F. J.; Civalleri, B.; Meyer, A.; Musto, P.; Albunia, A. R.; Rizzo, P.; Guerra, G. Normal Vibrational Analysis of the Syndiotactic Polystyrene s(2/1)2 Helix. *J. Phys. Chem. B* **2009**, *113*, 5059−5071.
(45) Torres, F. J.; Civalleri, B.; Pisani, C.; Musto, P.; Albunia, A. R.; Guerra, G. Normal Vibrational Analysis of a trans-Planar Syndiotactic Polystyrene Chain. *J. Phys. Chem. B* **2007**, *111*, 6327−6335.
(46) Ferrari, A. M.; Civalleri, B.; Dovesi, R. Ab Initio Periodic Study of the Conformational Behavior of Glycine Helical Homopeptides. *J. Comput. Chem.* **2010**, *31*, 1777−1784.
(47) Galimberti, D.; Quarti, C.; Milani, A.; Brambilla, L.; Civalleri, B.; Castiglioni, C. IR Spectroscopy of Crystalline Polymers from Ab Initio Calculations: Nylon 6,6. *Vib. Spectrosc.* **2013**, *66*, 83−92.
(48) Quarti, C.; Milani, A.; Castiglioni, C. Ab Initio Calculation of the IR Spectrum of PTFE: Helical Symmetry and Defects. *J. Phys. Chem. B* **2013**, *117*, 706−718.
(49) Milani, A.; Galimberti, D. Polymorphism of Poly(butylene terephthalate) Investigated by Means of Periodic Density Functional Theory Calculations. *Macromolecules* **2014**, *47*, 1046−1052.
(50) Milani, A. A Revisitation of the Polymorphism of Poly(butylene-2,6-naphthalate) from Periodic First-Principles Calculations. *Polymer* **2014**, *55*, 3729−3735.
(51) Galimberti, D.; Milani, A. Crystal Structure and Vibrational Spectra of Poly(trimethylene terephthalate) from Periodic Density Functional Theory Calculations. *J. Phys. Chem. B* **2014**, *118*, 1954−1961.
(52) Dovesi, R.; Orlando, R.; Erba, A.; Zicovich-Wilson, C. M.; Civalleri, B.; Casassa, S.; Maschio, M.; Ferrabone, M.; De La Pierre, M.; D'Arco, P.; et al. CRYSTAL14: A Program for the Ab Initio Investigation of Crystalline Solids. *Int. J. Quantum Chem.* **2014**, *114*, 1287−1317.
(53) Dovesi, R.; Saunders, V. R.; Roetti, C.; Orlando, R.; Zicovich-Wilson, C. M.; Pascale, F.; Civalleri, B.; Doll, K.; Harrison, N. M.; Bush, I. J.; et al. CRYSTAL14 User's Manual; University of Torino: Torino, Italy, 2014.
(54) Maschio, L.; Kirtman, B.; Rérat, M.; Orlando, R.; Dovesi, R. Ab Initio Analytical Raman Intensities for Periodic Systems through a Coupled Perturbed Hartree-Fock/Kohn-Sham Method in an Atomic Orbital Basis. I. Theory. *J. Chem. Phys.* **2013**, *132*, 164101.
(55) Maschio, L.; Kirtman, B.; Rérat, M.; Orlando, R.; Dovesi, R. Ab Initio Analytical Raman Intensities for Periodic Systems through a Coupled Perturbed Hartree-Fock/Kohn-Sham Method in an Atomic Orbital Basis. II. Validation and Comparison with Experiments. *J. Chem. Phys.* **2013**, *132*, 164102.
(56) Becke, A. Density-Functional Thermochemistry. III. The Role of Exact Exchange. *J. Chem. Phys.* **1993**, *98*, 5648−5652.
(57) Lee, C.; Yang, W.; Parr, R. Development of the Colle-Salvetti Correlation-Energy Formula into a Functional of the Electron Density. *Phys. Rev. B* **1988**, *37*, 785−789.
(58) Civalleri, B.; Zicovich-Wilson, C. M.; Valenzano, L.; Ugliengo, P. B3LYP Augmented with an Empirical Dispersion Term (B3LYP-D*) as Applied to Molecular Crystals. *CrystEngComm* **2008**, *10*, 405−410.
(59) Grimme, S. Accurate Description of van der Waals Complexes by Density Functional Theory Including Empirical Corrections. *J. Comput. Chem.* **2004**, *25*, 1463−1473.
(60) Grimme, S. Semiempirical GGA-type Density Functional Constructed with a Long-Range Dispersion Correction. *J. Comput. Chem.* **2006**, *27*, 1787−1799.
(61) Tkatchenko, A.; Scheffler, M. Accurate Molecular Van Der Waals Interactions from Ground-State Electron Density and Free-Atom Reference Data. *Phys. Rev. Lett.* **2009**, *102*, 073005.
(62) Ambrosetti, A.; Alfè, D.; DiStasio, R. A.; Tkatchenko, A. Long-range correlation energy calculated from coupled atomic response functions. *J. Chem. Phys.* **2014**, *140*, 18A508.
(63) Ambrosetti, A.; Reilly, A. M.; DiStasio, R. A.; Tkatchenko, A. Hard Numbers for Large Molecules: Toward Exact Energetics for Supramolecular Systems. *J. Phys. Chem. Lett.* **2014**, *5*, 849−855.
(64) Long, D. A. *The Raman Effect*; John Wiley & Sons, LTD: Chichester, U.K., 2002.
(65) Woodward, L. A. *Introduction to the Theory of Molecular Vibrations & Vibrational Spectroscopy*; Clarendon Press: Oxford, U.K., 1972.
(66) Merrick, J. P.; Moran, D.; Radom, L. An Evaluation of Harmonic Vibrational Frequency Scale Factors. *J. Phys. Chem. A* **2007**, *111*, 11683−11700.